

# UC Santa Barbara

## UC Santa Barbara Previously Published Works

### Title

Lasing emission of InGaAs quantum dot microdisk diodes

### Permalink

<https://escholarship.org/uc/item/7gh1649w>

### Journal

IEEE Photonics Technology Letters, 16(1)

### ISSN

1041-1135

### Authors

Zhang, L D

Hu, E

### Publication Date

2004

Peer reviewed

# Lasing Emission of InGaAs Quantum Dot Microdisk Diodes

Lidong Zhang and E. Hu, *Fellow, IEEE*

**Abstract**—An improved three-arm airbridge contacted microdisk diode structure is presented. Continuous-wave lasing from InGaAs quantum dot (QD) in a  $\sim 4\text{-}\mu\text{m}$ -diameter microdisks is reported with the threshold current  $\sim 40\ \mu\text{A}$  at  $T = 5\ \text{K}$ . With the increase of injection current, the QD's emission blueshifts due to the band-filling effect, while the laser mode peak redshifts by thermal effect. When the QD's gain spectra shift out of alignment with the lasing mode, the next available whispering gallery mode starts lasing from QD wetting layer. The thermal heating effect is discussed by investigating the modes redshift with respect to injection current.

**Index Terms**—Epitaxial growth, laser modes, laser resonators, quantum dots (QDs), semiconductor device fabrication, semiconductor lasers.

## I. INTRODUCTION

WHISPERING gallery mode (WGM) microdisks having high-quality factors and small modal volume have demonstrated exceedingly small thresholds [1], [2]. Incorporation of quantum dots (QDs) as the active medium promises enhanced performance because of their narrow spectral width and reduced absorption. We have recently reported a  $4\text{-}\mu\text{m}$ -diameter *electrically injected* QD microdisk laser with a threshold current of  $\sim 70\ \mu\text{A}$  [3]. This letter describes initial power-dependent measurements of the laser.

## II. GROWTH AND FABRICATION PROCESS

The materials used in this study were grown by a Varian Gen II molecular beam epitaxy (MBE) system with the layer structures given in Table I. The active GaAs disk region consists of two layers of InGaAs QDs (separated by an  $80\text{-}\text{\AA}$  GaAs spacer layer) and cladding layers of  $\text{Al}_x\text{Ga}_{1-x}\text{As}$ ,  $x = 0.3$  to better confine the optical field to the plane of the QDs. The QD's growth condition is described in [4]. Photoluminescence of the as-grown QD's material reveals a broad peak ranging from  $900\text{--}990\ \text{nm}$ . The areal dot density for each QD layer was calibrated to be  $3 \times 10^{10}\ \text{cm}^{-2}$  using atomic-force microscopy on uncapped islands grown under the same growth conditions.

Optical lithography and selective wet etching were used to form the double-disk structures shown schematically in

Manuscript received November 13, 2002; revised May 5, 2003. This work was supported by ARO DARPA MDA972-01-1-0027 and DARPA/QUIST 8-447800-23140-2. This work made use of MRL Central Facilities supported by the MRSEC Program of the National Science Foundation under Award DMR00-80034.

The authors are with the Department of Electrical and Computer Engineering, University of California, Santa Barbara, CA 93106 USA (e-mail: lidong@engineering.ucsb.edu).

Digital Object Identifier 10.1109/LPT.2003.818920

TABLE I  
EPITAXIAL LAYER STRUCTURES GROWN BY MBE

Material	Thickness	Impurity concentration ( $\text{cm}^{-3}$ )
GaAs	1000 $\text{\AA}$	p, $\sim 2 \times 10^{19}$
$\text{Al}_x\text{Ga}_{1-x}\text{As}$ , $x=0.7$	0.2 $\mu\text{m}$	p, $\sim 5 \times 10^{18}$
GaAs	100 $\text{\AA}$	p, $\sim 5 \times 10^{18}$
$\text{Al}_x\text{Ga}_{1-x}\text{As}$ , $x=0.3$	200 $\text{\AA}$	p, $0\text{--}5 \times 10^{18}$
GaAs	700 $\text{\AA}$	uid
2x { InAs QD layers / GaAs spacer }	2x { $\sim 80\ \text{\AA}$ }	uid
GaAs	700 $\text{\AA}$	uid
$\text{Al}_x\text{Ga}_{1-x}\text{As}$ , $x=0.3$	200 $\text{\AA}$	n, $5 \times 10^{18}\text{--}0$
GaAs	100 $\text{\AA}$	n, $\sim 5 \times 10^{18}$
$\text{Al}_x\text{Ga}_{1-x}\text{As}$ , $x=0.75$	$\sim 0.5\ \mu\text{m}$	n, $\sim 5 \times 10^{18}$
GaAs substrate and buffer layers	-	n, $1 \times 10^{19}$

Fig. 1(a). The top surface of the lower disk is doped p-type, while the bottom surface is doped n-type. These doped regions act as current spreading layers, so that carriers will be more easily captured by the QDs near the disk perimeter, where the low radial order ( $n \sim 1$ ) of WGMs propagates. The circular AlGaAs posts are formed by selective undercut etching in an HF-based etchant, which produces an upper post ( $\text{Al}_x\text{Ga}_{1-x}\text{As}$ ,  $x = 0.7$ ) with diameter larger than the lower post ( $\text{Al}_x\text{Ga}_{1-x}\text{As}$ ,  $x = 0.75$ ). Ti-Pt-Au air-bridges form the contact to the p-layer disk and Ni-AuGe-Ni-Au forms the n-type contacts. The device was annealed at  $430\ \text{^\circ C}$ , and we used test structures to determine the room temperature specific contact resistance for the n-type and p-type contacts to be  $\sim 1 \times 10^{-6}\ \Omega\ \text{cm}^2$ , and  $\sim 5 \times 10^{-6}\ \Omega\ \text{cm}^2$ , respectively. Fig. 1(b) is a scanning electron microscope image of a  $\sim 4\text{-}\mu\text{m}$ -diameter device similar to the ones studied in this letter. The upper-left inset displays the airbridge structure used for calibrating p-contact resistance. Further details of the structure fabrication may be found in [3].

The devices are Au wire bonded and are mounted in a Janis closed-cycle Helium cryostat and cooled to 5 K. We swept the bias voltage to inject current into the device and collected the electroluminescence from the microdisk edge by a spectrometer connected with a liquid  $\text{N}_2$  cooled Si charged-coupled device (CCD) camera.

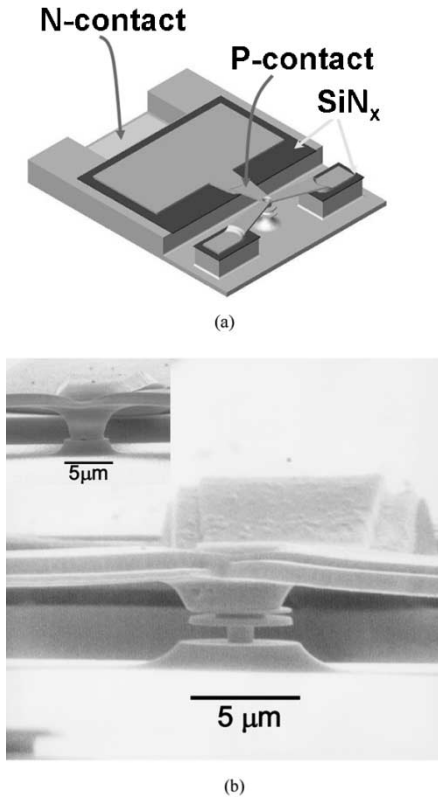


Fig. 1. (a) Schematic illustration of the three-arm airbridge contacted microdisk diode structure. Top p-contact on the upper disk is made by fabricating a Ti–Pt–Au metal airbridge for carrier injection. N-contact is Ni–AuGe–Ni–Au. (b) Scanning electron microscope image of a  $\sim 4\text{-}\mu\text{m}$ -diameter double disk microdisk diode device. The upper-left inset: the airbridge structure for calibrating p-contact resistance.

### III. RESULTS AND DISCUSSION

Microdisks with 3–5- $\mu\text{m}$  diameters were formed in this study. We observe that for a 4- $\mu\text{m}$ -diameter disk, if the upper post is larger than 3  $\mu\text{m}$  in diameter, no WGMs are observed. The device behaves like a light-emitting diode, showing a continuous quasi-linear increase of intensity of broad emission from the QD ensemble that is gradually blueshifted with increased injection current. We carried out a finite-difference time-domain (FDTD) simulation of a 4- $\mu\text{m}$ -diameter microdisk to determine the electromagnetic field distributions of the first-order ( $n = 1$ ) WGMs with frequencies overlapping with the QD spectral range. The modes are confined within a ring of 0.5  $\mu\text{m}$  from the disk perimeter. The loss introduced by the overlap of the upper post material with the microdisk precludes the observation of the high- $Q$  WGMs. When the upper post diameter is smaller than 2.7  $\mu\text{m}$ , the device demonstrates lasing.

Fig. 2 displays the light output–current curve for a  $\sim 4\text{-}\mu\text{m}$ -diameter QDs microdisk laser, with a threshold current deduced to be 43–50  $\mu\text{A}$  and emission wavelength of 920 nm. Assuming a uniform current distribution from the post to the disk edge, we estimate that  $J_{th} = 342\text{ A/cm}^2$ . The inset of Fig. 2 displays the laser spectra taken at various injection currents ( $I$ ), where the current varies from below threshold to twice the threshold current, respectively. Our FDTD analysis identifies the 920-nm transition to be TE( $n, m$ ) mode = TE(1, 38), where  $n$  and  $m$  are the radial and azimuthal mode numbers, respectively. As we

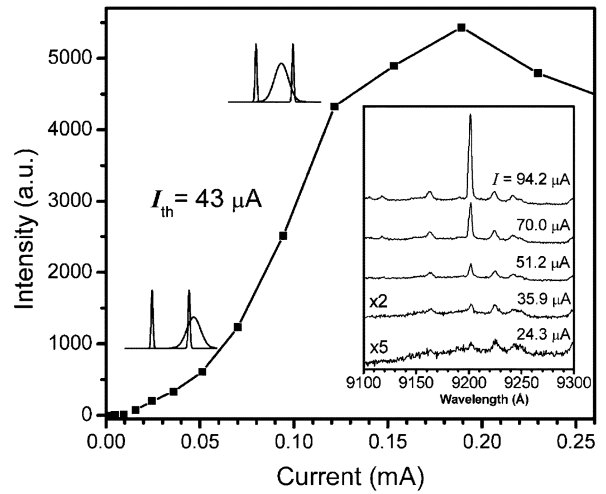


Fig. 2. Measured light output from the laser mode at 920 nm as a function of current  $I$ . Threshold current is  $I_{th} = 43\text{--}50\ \mu\text{A}$ . Measurements were performed at  $T = 5\text{ K}$  on a  $\sim 4\text{-mm}$ -diameter microdisk laser in cw operation. The inset displays the lasing spectra evolution.

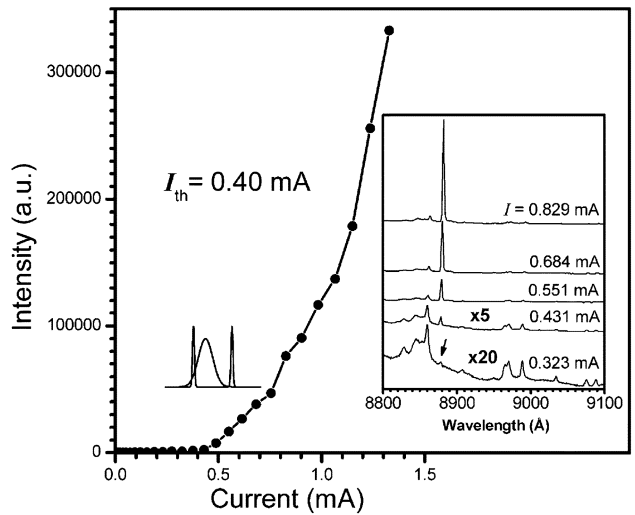


Fig. 3. Measured light output from the laser mode at 888 nm as a function of current  $I$  of the same microdisk diode as Fig. 2. Threshold current is  $I_{th} = 0.4\text{ mA}$ . The inset displays the lasing spectra evolution.

continue to increase the injection current, the intensity of the 920-nm peak begins to decrease, and lasing at  $\lambda = 887.9\text{ nm}$  dominates. This is shown in the inset of Fig. 3; the threshold current for this peak is  $\sim 0.4\text{ mA}$ . FDTD simulations identify the TE (1, 40) to be at 888 nm. We believe that this lasing transition results from the overlap of the broad emission from the wetting layer with this WGM. Similar lasing characteristics are observed in other microdisks.

Fig. 4 shows the wavelength shift of the lasing transitions as a function of injection power. As the injection current is increased from 20 to 430  $\mu\text{A}$ , the 920-nm peak shifts by only 0.07 nm and no shifts are observed for the 888-nm mode. At high injection currents, both the 920- and 888-nm peaks undergo a redshift, which we estimate from Fig. 4 to be  $(d\lambda/dP) = 0.37\text{ nm/mW}$ . The changes in the lasing peak and the redshifts are believed to be evidence of heating of the microdisk at high injection currents. We expect that the temperature-dependent change in the

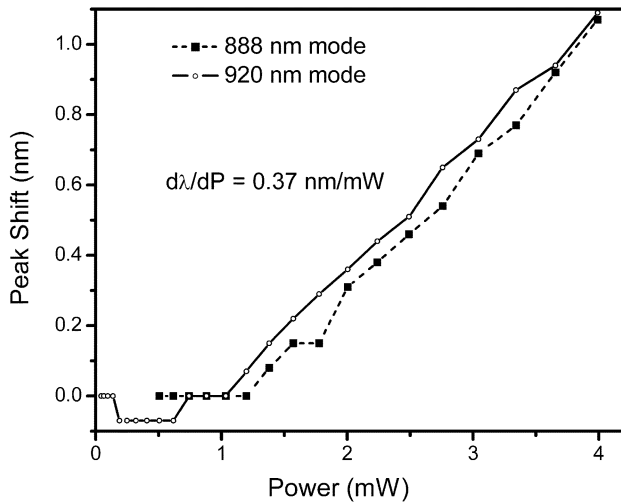


Fig. 4. Measured change in wavelength versus dissipated power for both laser modes of 888 and 920 nm.

QD emission peak is far greater than the temperature dependency of the mode position. In fact, Imamoglu *et al.* used this differential temperature dependence to tune a QD transition into resonance with the cavity mode for structures similar to those described here [5]. At low temperatures ( $<20$  K), mode shift versus temperature  $dE_{\text{WGM}}/dT$  is estimated to be  $<5 \mu\text{eV/K}$ . This corresponds to our observation that no significant peak shifts occurred at low injection levels, implying that the temperature change induced by current heating was less than 15 K. While the slight shift in the WGMs is due to a change in refractive index with temperature, the change in the QD emission peak position is due to the temperature-dependent shrinkage in bandgap for GaAs and InGaAs, which is about an order of magnitude higher. Consequently, the peak change data in Fig. 4 provide insight into the device heating and the temperature rise in the device can be deduced quantitatively by comparing the WGM redshift results in [5]. At high injection levels, the WGM position deviation of 0.5 nm indicates a temperature change as large as 30 K.

We thus postulate the following behavior for the microdisk operation. At low injection powers, several peaks appear, but as we increase the injection current, only the 920-nm peak achieves lasing. The predominance of the single lasing transition for injection currents up to 0.3 mA suggests that it is only for QDs emitting at that frequency that there is sufficient spatial overlap between the QD emitters and the antinodes of the WGM. As the injection current continues to increase, some heating of the microdisk takes place, and the QD emission frequency begins to shift away from peak position of the WGM. We observed that the electroluminescence intensity increases with higher injection current, and the peak of the broad spectrum blueshifts, due to band-filling that occurs at higher injection currents [6]–[8]. This results in the gradual reduction of peak intensity at  $I > 0.2$  mA. At even higher injection current, substantial transitions are excited in the wetting layer, which is characterized by a broad peak in the region of about 880 nm. The overlap

of the wetting layer transition with the WGM in the spectral region induces lasing at 888 nm, which dominates the lasing spectrum. Further, we can use our FDTD simulation to estimate the magnitude of the refractive index change  $\Delta n$  and, hence, the local temperature rises. For a specific WGM, we obtain  $\Delta n = 4.3 \times 10^{-3}$  for a redshift of  $\Delta\lambda = 1$  nm. Using an expression for the dependence of the refractive index on temperature [7],  $\Delta n(\Delta T) = \beta_{\text{disk}} \Delta T$ , we can deduce the temperature coefficient  $\beta_{\text{disk}} \sim 7 \times 10^{-5} \text{K}^{-1}$  for our structure from Fig. 4. Note that a larger value is quoted for bulk GaAs,  $\beta_{\text{GaAs}} \sim 4 \times 10^{-4} \text{K}^{-1}$  [9].

#### IV. CONCLUSION

We have fabricated an airbridge-contacted microdisk laser structure with QD active region. Continuous-wave lasing of 920 nm from  $\sim 4\text{-}\mu\text{m}$ -diameter InGaAs QDs ( $\sim 6 \times 10^{10}/\text{cm}^2$ ) microdisks is reported with the threshold current around  $40 \mu\text{A}$  at  $T = 5$  K. With increased injection current, the QD spectrum blueshifts due to band-filling effects; higher injection currents also give rise to thermal heating, resulting in the gain peak shifting out of alignment with the laser mode of 920 nm, the next mode at 888 nm starts lasing from QD wetting layer. The temperature change in the device is investigated by the peak redshifts at higher injection levels.

#### ACKNOWLEDGMENT

The authors would like to thank Prof. A. Imamoglu, A. Kiraz, and J. Urayama for enlightening discussions and for assistance in some of the optical measurements in this work. The authors also thank Prof. J. Bowers and Prof. A. Gossard for their encouragement and valuable discussion.

#### REFERENCES

- [1] H. Cao, J. Y. Xu, W. H. Xiang, Y. Ma, S. H. Chang, S. T. Ho, and G. S. Solomon, "Optically pumped InAs quantum dot microdisk lasers," *Appl. Phys. Lett.*, vol. 76, pp. 3519–3521, 2000.
- [2] P. Michler, A. Kiraz, L. Zhang, C. Becher, E. Hu, and A. Imamoglu, "Laser emission from quantum dots in microdisk structures," *Appl. Phys. Lett.*, vol. 77, pp. 184–186, 2000.
- [3] L. Zhang and E. Hu, "Lasing from InGaAs quantum dots in an injection microdisk," *Appl. Phys. Lett.*, vol. 82, pp. 319–321, 2003.
- [4] J. M. Garcia, T. Mankad, P. O. Holtz, P. J. Wellman, and P. M. Petroff, "Electronic states tuning of InAs self-assembled quantum dots," *Appl. Phys. Lett.*, vol. 72, pp. 3172–3174, 1998.
- [5] A. Kiraz, P. Michler, C. Becher, B. Gayral, A. Imamoglu, L. Zhang, E. Hu, W. V. Schoenfeld, and P. M. Petroff, "Cavity-quantum electrodynamics using a single InAs quantum dot in a microdisk structure," *Appl. Phys. Lett.*, vol. 78, pp. 3932–3934, 2001.
- [6] D. L. Huffaker and D. G. Deppe, "Electroluminescence efficiency of 1.3  $\mu\text{m}$  wavelength InGaAs/GaAs quantum dots," *Appl. Phys. Lett.*, vol. 73, pp. 520–522, 1998.
- [7] C. Ribbat, S. Bognar, R. Sellin, and D. Bimberg, "Spectral mode dynamics of short cavity quantum-dot lasers," *Appl. Phys. Lett.*, vol. 81, pp. 147–149, 2002.
- [8] M. Fujita, R. Ushigome, and T. Baba, "Large spontaneous emission factor of 0.1 in a microdisk injection laser," *IEEE Photon. Technol. Lett.*, vol. 13, pp. 403–405, May 2001.
- [9] J. Piprek, H. Wenzel, and G. Sztetka, "Modeling thermal effects on the light vs. current characteristic of gain-guided vertical-cavity surface-emitting lasers," *IEEE Photon. Technol. Lett.*, vol. 6, pp. 139–142, Feb. 1994.